

Ferroelectric polarization switching induced from water adsorption in BaTiO₃ ultrathin filmsPierre-Marie Deleuze , Bruno Domenichini , and Céline Dupont **Laboratoire Interdisciplinaire Carnot de Bourgogne, UMR 6303, CNRS, Université de Bourgogne Franche Comté, Boîte Postale 47870, 21078 Dijon Cedex, France*

(Received 24 October 2019; revised manuscript received 14 January 2020; accepted 17 January 2020; published 7 February 2020)

The influence of water on the out-of-plane polarization of BaTiO₃ (BTO) ultrathin films is studied by means of density functional theory calculations. The adsorption is investigated for different coverages on both terminations of BTO with, for each case, all possible states of polarization, namely, paraelectric, polarized upward, and polarized downward. We thus demonstrate different behavior as a function of the termination. While H₂O adsorbs only dissociatively on the BaO termination, with a reinforced interaction compared to BTO without out-of-plane polarization, only molecular adsorption is observed on the TiO₂ termination. In addition, the presence of water is able to switch the polarization. Whatever the initial state of polarization is, water induces a downward state on the BaO termination and an upward polarization on the TiO₂ one. A detailed analysis of this phenomenon is given.

DOI: [10.1103/PhysRevB.101.075410](https://doi.org/10.1103/PhysRevB.101.075410)**I. INTRODUCTION**

Among the large family of metal oxides, ferroelectric materials have lately received a lot of attention as potential photocatalysts [1–3]. Indeed, their permanent intrinsic polarization allows to properly align bands instead of using an external electric bias and enables photocarrier separation, limiting electron-hole recombination, one of the major drawbacks of oxides [4]. However, the existence of polarization cannot be neutral in reaction conditions. In particular the influence of polarization on the interaction of molecules with ferroelectric surfaces has been widely studied. The case of P^+ and P^- surfaces of LiNbO₃(0001) has been considered both experimentally [5,6] and theoretically [7,8] for their interaction with either H₂O, CH₃OH, or H and OH radicals. In all of these cases, different interactions have been evidenced depending on the P^+ or P^- surface. Other classical ferroelectrics like BaTiO₃ [9–11], Pb(Zr_{0.8}Ti_{0.2})O₃ [9], and PbTiO₃ [12] have been studied, always with the same conclusions: there is a correlation between the oxide polarization and the surface interactions. This difference in behavior as a function of the polarization has opened the door to switchable chemistry [3,13]. In fact, by imposing an external potential able to switch from P^+ to P^- or vice versa, one can benefit from the physical and chemical properties of each surface. Beyond the electrical switching, the chemical switching was first evidenced in 2009 by Wang *et al.* for PbTiO₃ in the presence of O₂ [14]. Following this paper, several studies [15–19] focused on the surface charge screening potentially leading to a reversal of the surface dipole. Despite the great importance of this phenomenon and potential applications, up to now no study has described the interaction of water with one of the most important ferroelectric materials, BaTiO₃

(BTO) presenting an out-of-plane polarization. Theoretically, only studies [20–22] describing water adsorption on in-plane polarized BaTiO₃ have been conducted.

Thus, in this paper we endeavor to thoroughly describe the interaction of H₂O with both TiO₂ and BaO terminations of out-of-plane polarized ultrathin BaTiO₃.

II. COMPUTATIONAL DETAILS

Calculations were performed in the framework of the density functional theory (DFT) using the Vienna *Ab initio* Simulation Package (VASP) code [23,24]. Because the long-range van der Waals interactions play an important part in the interaction between water and the BaTiO₃ surface, calculations were made using the dispersion-corrected density functional theory (DFT-D3) [25]. The electronic-exchange correlation potential was treated using the generalized gradient approximation with the Perdew-Burke-Ernzerhof [26] functional. Pseudopotentials of the projector augmented wave [27,28] were employed and included 10 valence electrons for Ba ($5s^2 5p^6 4s^2 3d^2$), 6 for O ($2s^2 2p^4$), and 12 for Ti ($3s^2 3p^6 4s^2 3d^2$). The plane wave energy cutoff was set to 500 eV. The Coulomb interaction $U_{\text{eff}} = 3.5$ eV was applied to Ti $3d$ electrons.

The tolerance of the total energy convergence was set to 10^{-6} eV. The structural relaxation was carried out until all the forces on the atoms converged below 0.01 eV/Å. In the following, different periodicities N of unit cells are considered to modify the water coverage; a $7 \times 7 \times 1$ Monkhorst-Pack [29] k -point mesh was used to sample the first Brillouin zone for the smallest periodicity ($N = 2$). For larger cells, the grid was adapted accordingly.

BTO is often deposited on a substrate like Pt. However, we calculated that, beyond the induced strain, the presence of the substrate has no influence on the water adsorption. Nevertheless, the presence of platinum is considered through

*celine.dupont@u-bourgogne.fr

the 2.1% compressive strain imposed on BTO by the lattice mismatch between Pt and BTO. Hence, in the following, platinum is not implemented explicitly. However, to support our choice, for each configuration of isolated strained BTO reported in this paper, the equivalent structure with an explicit platinum substrate is reported in the Supplemental Material [30]. In the following, BTO surfaces are thus modeled by symmetric TiO_2 -terminated and BaO-terminated surfaces of 11 layers, in which all atoms are free to relax, allowing a complete and free optimization of the slab polarization. This model corresponds to an ultrathin film with a thickness of 2.1 nm, which has been evidenced as sufficient for the appearance of ferroelectricity, both experimentally [31,32] and theoretically [33]. In addition, we checked that higher thickness leads to the same polarization patterns (see Fig. S11 in the Supplemental Material). A vacuum layer of 20 Å is implemented to prevent any interactions between periodic images along the z direction. The method used to model the out-of-plane polarization is extensively described elsewhere [33]. In summary, it follows Migoni's [34] approach, which consists of dividing the slab into two domains of opposite polarization, leading to an overall cell with no net dipole moment.

When a single water molecule is adsorbed on the surface, the adsorption energy is defined as

$$E_{\text{ads}} = E(\text{slab} + \text{H}_2\text{O}) - E(\text{slab}) - E(\text{H}_2\text{O}), \quad (1)$$

where $E(\text{slab} + \text{H}_2\text{O})$ is the total energy of the optimized slab with one water molecule adsorbed, $E(\text{slab})$ is the total energy of the optimized paraelectric slab without water, and $E(\text{H}_2\text{O})$ is the total energy of the free water molecule. Therefore, a negative value of E_{ads} means that the adsorption is favorable.

When two water molecules are adsorbed, depending on the nature of the adsorption, either both adsorption energies are treated separately, or the average adsorption energy is considered. In the first case, the adsorption energy of the first molecule is calculated with Eq. (1), and the value is referred to as E_{ads}^1 . The adsorption energy of the second molecule is calculated as

$$E_{\text{ads}}^2 = E(\text{slab} + 2\text{H}_2\text{O}) - E(\text{slab} + \text{H}_2\text{O}) - E(\text{H}_2\text{O}), \quad (2)$$

where $E(\text{slab} + 2\text{H}_2\text{O})$ is the total energy of the optimized slab with two water molecules adsorbed, $E(\text{slab} + \text{H}_2\text{O})$ is the total energy of the optimized slab with a single water molecule, and $E(\text{H}_2\text{O})$ is the total energy of the free water molecule.

In the following, the length of the elongated O-H of the water molecule is called OH_W , while the distance between the surface oxygen and the hydrogen of the water molecule is named OH_S , as described in Fig. 1.

III. RESULTS

A. Adsorption modes

1. BaO termination

The adsorption of water is first considered on the BaO termination, for coverages ranging from 1/8 to 1/2 monolayer (ML). All stable configurations are named as follows: X_θ^N , where θ refers to the coverage (1/8, 1/4, or 1/2 ML), N

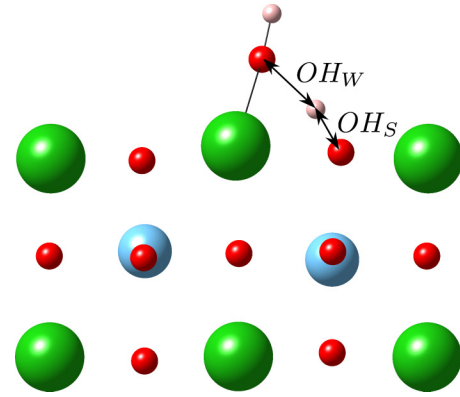


FIG. 1. Side view of the first three layers of a BaO-terminated slab with a water molecule adsorbed. Characteristic distances OH_W and OH_S are represented. Ba atoms are in green, Ti atoms are in blue, oxygen atoms are in red, and hydrogen atoms are in white.

refers to the periodicity (two or four unit cells), and X allows for different configurations of the same θ and N and takes values A, B, C, \dots . For the lowest coverage (1/8 ML) one water molecule is adsorbed in a cell with a lateral periodicity of four unit cells ($N = 4$). As an initial state, different geometrical configurations of the water molecule are combined with different states of polarization, namely, the paraelectric slab and the upward and the downward polarized part of the slab. Figure 2 shows the two obtained stable configurations, while their corresponding adsorption energies are reported in Table I. For the sake of clarity, only the three upper cells are reported, while the whole simulation cell composed of five unit cells is represented in the Supplemental Material. As shown in Fig. 2, the final state always presents a downward

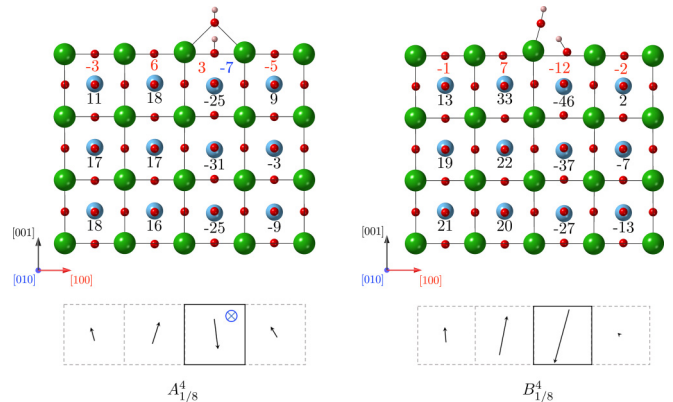


FIG. 2. Top: Side views of the most stable structures of the BaO-terminated surface with a four-unit-cell periodicity ($N = 4$) for a $\frac{1}{8}$ -ML adsorption. Only the first seven layers are represented. The values in black, blue, and red indicate the polarization (in $\mu\text{C}/\text{cm}^2$) in each unit cell along the [001], [010], and [100] directions, respectively. Only nonzero polarization is shown. See Fig. S12 in the Supplemental Material for the representation of the whole simulation cell. Bottom: Vectorial representation of the polarization in the cells of the first layer. Cells with water adsorbed on their surface are represented by solid lines, while cells without water are shown by dotted lines. In this and subsequent figures, a blue circled cross or dot indicates the existence and direction of polarization along the [010] axis.

TABLE I. Water adsorption energies (in eV) on a BaO termination as a function of the water coverage. As previously described, E_{ads}^1 refers to the adsorption energy of the first water molecule, and E_{ads}^2 refers to the addition of a second water molecule. When both water molecules are equivalent, only the average adsorption energy is given.

Coverage	Periodicity	Configuration	E_{ads}^1	E_{ads}^2	
$\frac{1}{8}$ ML	$N = 4$	$A_{1/8}^4$	-1.12		
		$B_{1/8}^4$	-1.15		
$\frac{1}{4}$ ML	$N = 2$	$A_{1/4}^2$	-1.09		
		$B_{1/4}^2$	-1.08		
		$N = 4$	$A_{1/4}^4$	-1.07	
		$B_{1/4}^4$	-1.08		
		$C_{1/4}^4$	-1.04		
		$D_{1/4}^4$	-1.09		
		$E_{1/4}^4$	-1.15	-0.95	
		$F_{1/4}^4$	-1.12	-0.96	
	$G_{1/4}^4$	-1.15	-0.97		
$\frac{1}{2}$ ML	$N = 2$	$A_{1/2}^2$	-1.09	-0.90	
		$B_{1/2}^2$	-1.08	-0.96	
		$C_{1/2}^2$	-1.09	-0.79	

polarization regardless of the initial polarization. These important findings will be discussed in detail later.

In both cases, water spontaneously dissociates into a H^+ ion, which bonds with a surface oxygen, and a hydroxyl group that binds between two Ba atoms in either the (100) or (010) plane (see Fig. 2), referred to as $A_{1/8}^4$ and $B_{1/8}^4$, with adsorption energies of -1.15 and -1.12 eV, respectively. In the following, whatever the coverage is, the adsorption with a configuration similar to $A_{1/8}^4$ will be referred as mode 1, while adsorption similar to $B_{1/8}^4$ will be called mode 2. In $A_{1/8}^4$, the OH_S distance is 1.05 Å, and OH_W is 1.48 Å, while in $B_{1/8}^4$ OH_S and OH_W are 1.02 and 1.57 Å, respectively. These findings compare very well with previous results. In fact, our $A_{1/8}^4$ configuration corresponds to the dissociative adsorption observed by Geneste and Dkhil [20], without out-of-plane polarization. Nevertheless, they obtained a lower adsorption energy of -0.77 eV. If our higher adsorption can be partially explained by our level of calculation (we have included dispersion corrections which reinforce hydrogen bonds), this correction is not sufficient to justify the difference of 0.35 eV. Indeed, without dispersion corrections, the adsorption energy of $A_{1/8}^4$ is reduced from -1.12 to -0.98 eV, a value still 0.21 eV higher than the one on BTO without out-of-plane polarization. Hence, the out-of-plane polarization clearly reinforces the interaction between water and BTO. This can also explain why we observe only dissociated water on the BaO termination, while previous studies [20,21], without out-of-plane polarization or inclusion of dispersion, were able to stabilize molecular H_2O on BaO. In this spirit, the molecular adsorption state found by Geneste and Dkhil [20] with an adsorption energy of -0.72 eV can be seen as a precursor of our dissociated $B_{1/8}^4$ configuration.

The coverage was then increased to $1/4$ ML in two different ways: either by adding a second molecule to the $1/8$ -ML case or by considering a single water molecule

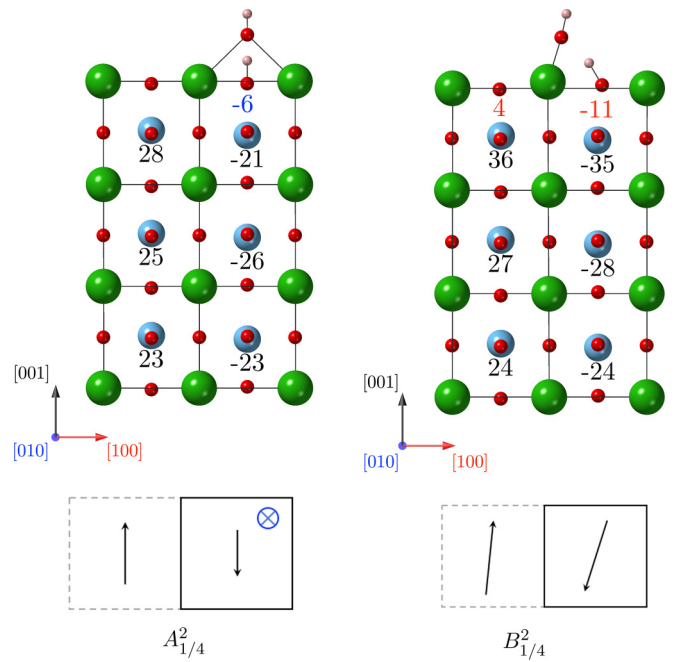


FIG. 3. Most stable structures of the BaO-terminated surface with $N = 2$ and $\theta = \frac{1}{4}$ ML. See Fig. SI3 in the Supplemental Material for the representation of the whole simulation cell.

in a cell with a lateral periodicity of two unit cells ($N = 2$). The latter case is very similar to the $1/8$ -ML coverage already discussed. The obtained configurations are reported in Fig. 3, and adsorption energies are given in Table I. The only difference from $\theta = 1/8$ ML lies in the adsorption energy, which is a bit reduced for this higher coverage: values of -1.09 and -1.08 eV are obtained at $\theta = 1/4$ ML, instead of -1.15 and -1.12 eV, respectively, for $\theta = 1/8$ ML as a consequence of lateral interactions. For $\theta = 1/4$ ML obtained through the adsorption of two water molecules in the larger cell ($N = 4$), there are more cases: the second molecule can be added either on the same unit cell as the first one or on another unit cell, adjacent or not. The most stable configurations can be divided in two categories depending on whether the second molecule dissociates (Fig. 4) or not (Fig. 5). The obtained results suggest that water is more inclined to dissociate, as previously observed [21]. Nevertheless, the adsorption energies in the mixed adsorption structures are very close, so each configuration is likely to exist. If the second water molecule adsorbs on the surface without interacting with the first one, it spontaneously dissociates in the same geometry as the previously observed structures (modes 1 and 2). In the mixed adsorption case (see Fig. 5), the second water molecule maintains its molecular state and forms a hydrogen bond with the first water molecule. The length of the hydrogen bond is 1.59 Å in $E_{1/4}^4$ and 1.52 Å in $F_{1/4}^4$. This interaction causes the first molecule to be even more distorted. Indeed, in $E_{1/4}^4$ OH_W stretches from 1.57 to 1.99 Å, and it stretches from 1.48 to 1.65 Å in $F_{1/4}^4$. Moreover, in $E_{1/4}^4$ the second water molecule through the hydrogen bond pulls the first dissociated water molecule. Thus, the second hydrogen bond (OH_W) pulls the O ion out from the surface by 0.52 Å, which induces a very large out-of-plane polarization in the first surface layers. In

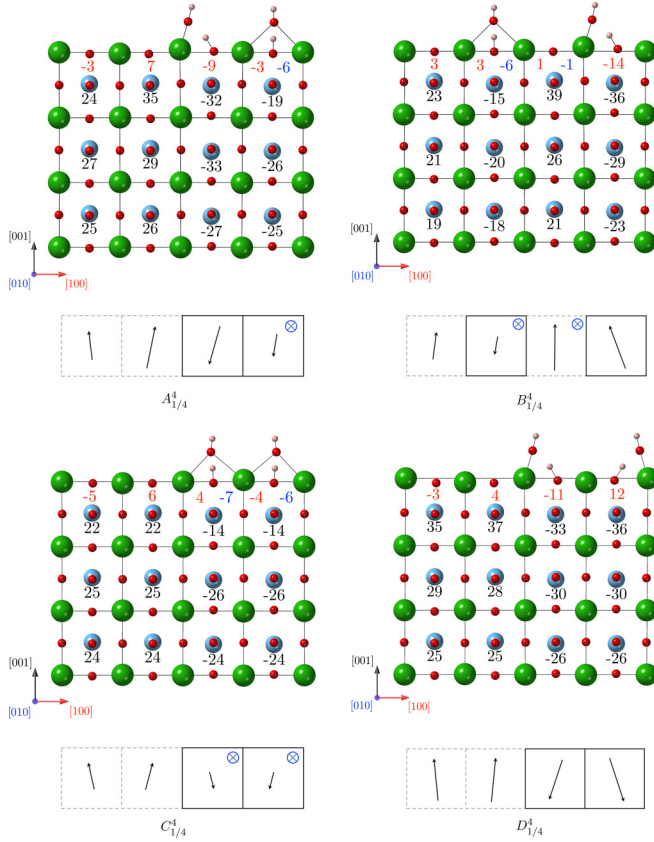


FIG. 4. Most stable structures of dissociated water on the BaO-terminated surface with $N = 4$ and $\theta = \frac{1}{4}$ ML. See Fig. S14 in the Supplemental Material for the representation of the whole simulation cell.

$G_{1/4}^4$, the second water molecule is adsorbed in a configuration similar to mode 2 but less bonded to the surface, leading to a nondissociated configuration. Hence, $d(\text{Ba-O})$ is extended to 3.01 Å instead of 2.71 Å, and OH_S is not a real O-H bond like in mode 2, where $d(\text{O-H}) = 1.02$ Å, but a hydrogen bond of 1.47 Å.

Finally, the highest considered coverage is half a monolayer. To reach such a coverage, a second water molecule is added to $\theta = 1/4$ ML in the $N = 2$ periodicity. The obtained structures are shown in Fig. 6. In all cases, the second water molecule adsorbs molecularly on the surface. However, the adsorption is more favorable when both molecules are on the same downward polarized domain. In such a case, the interaction between the two molecules leads to a larger distortion of the first molecule as OH_W stretches from 1.45 to 1.60 Å in $A_{1/2}^2$ and from 1.52 to 1.61 Å in $B_{1/2}^2$. This behavior was already observed by Li *et al.* when studying water adsorption on in-plane polarized BTO [21].

2. TiO_2 termination

Let us now discuss the behavior of water adsorption on the TiO_2 termination. We consider the same coverages as before, with water initially adsorbed either on the upward or the downward polarized domain as well as on the paraelectric slab. On TiO_2 , whatever the starting polarization, only the upward slab is obtained as a final state. This result will be

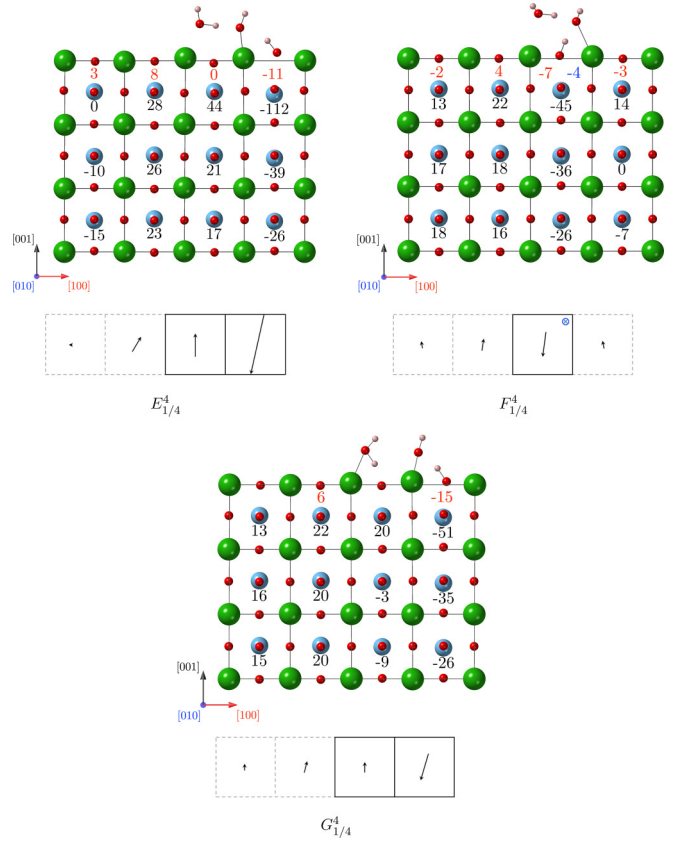


FIG. 5. Most stable structures of the mixed adsorption cases on the BaO-terminated surface with $N = 4$ and $\theta = \frac{1}{4}$ ML. See Fig. S15 in the Supplemental Material for the representation of the whole simulation cell.

discussed later. The obtained configurations are reported in Figs. 7 and 8, with their corresponding energies given in Table II.

Contrary to what occurs on BaO, water adsorbs only molecularly on TiO_2 without spontaneous dissociation, whatever the coverage is. This indicates a weaker interaction with the TiO_2 termination, confirmed by a lower adsorption energy of -0.97 eV instead of -1.14 eV on BaO. This is in agreement with previous findings on in-plane polarized BTO [20,21] and also on $\text{SrTiO}_3(001)$ [35], meaning that out-of-plane polarization does not dramatically influence the adsorption modes.

At the highest coverage ($\theta = 1/2$ ML; Fig. 8), the second molecule can adsorb either on the same domain as the first

TABLE II. Water adsorption energies in eV on TiO_2 termination as a function of the water coverage.

Coverage	Periodicity	Configuration	E_{ads}^1	E_{ads}^2
$\frac{1}{8}$ ML	$N = 4$	$A_{1/8}^4$	-0.98	
$\frac{1}{4}$ ML	$N = 2$	$A_{1/4}^2$	-0.97	
	$N = 4$	$A_{1/4}^4$		-0.97
$\frac{1}{2}$ ML	$N = 2$	$A_{1/2}^2$	-0.97	-0.99
		$B_{1/2}^2$		-0.94

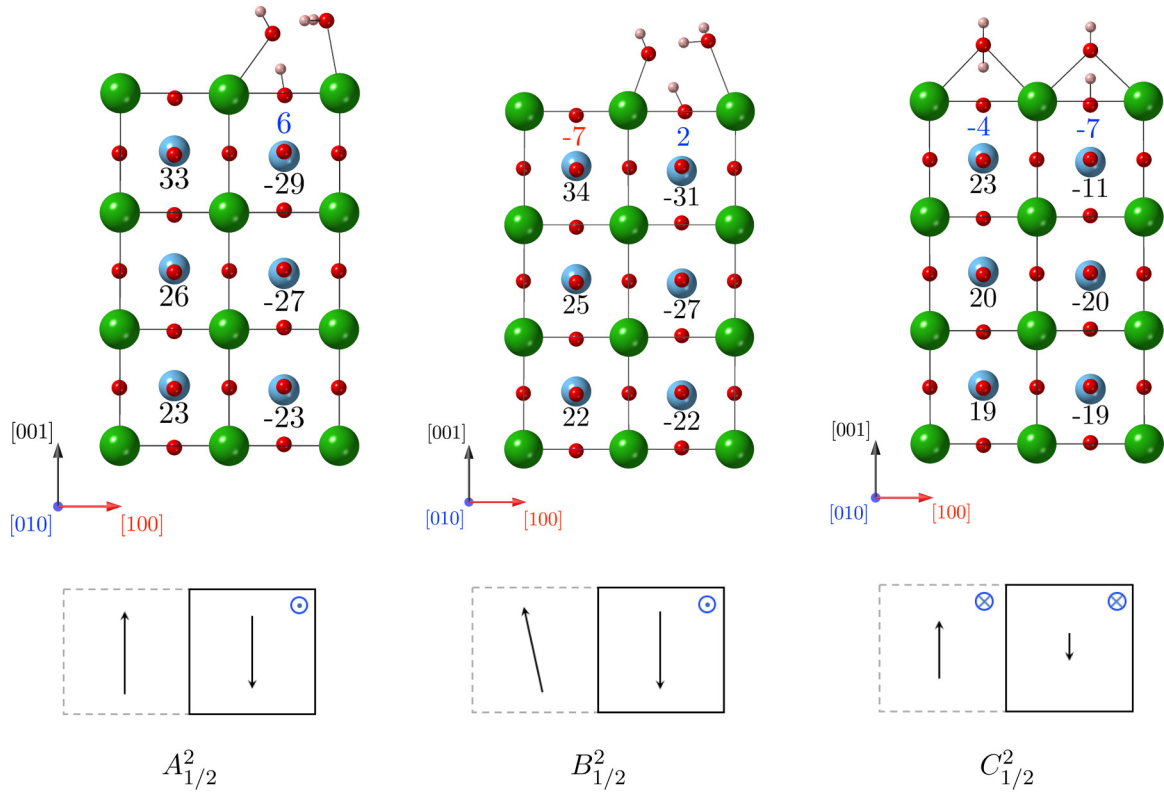


FIG. 6. Most stable structures of the BaO-terminated surface with $N = 2$ and $\theta = \frac{1}{2}$ ML. See Fig. SI6 in the Supplemental Material for the representation of the whole simulation cell.

one ($A_{1/2}^2$) or on the oppositely polarized domain ($B_{1/2}^2$). In the former case, the second molecule adsorbs through two hydrogen bonds: one with the first molecule and a second with the surface oxygen at a distance of 1.43 and 1.97 Å, respectively. The adsorption energy of the second water molecule is -0.99 eV in $A_{1/2}^2$, while the average adsorption energy in $B_{1/2}^2$ is -0.97 eV, indicating that both configurations can exist, with the single consequence being on the polarization, which will be discussed in the following.

For the sake of completeness, even if water does not dissociate spontaneously, the dissociated adsorption has been studied for the intermediate coverage of $1/4$ ML. The related configuration is reported in Fig. 9. This dissociation creates two OH groups, both oriented in the $[010]$ direction. The OH adsorbed on Ti pulls this Ti atom out of the surface by 0.61 Å. This causes large consequences for the polarization, which will be discussed later. From the energetic point of view, this dissociated case presents an adsorption energy of -1.28 eV, hence 0.3 eV stabler than the molecular adsorption. The dissociation barrier was roughly estimated at 0.1 eV through Climbing Image Nudged Elastic Band (CI-NEB) calculations [36], meaning that in real conditions we will more likely observe dissociated H_2O .

B. Polarization

The influence of water adsorption on the polarization is now discussed in detail. The first and most important conclusion concerns the global polarization. In fact, whatever the initial state (paraelectric or polarized upward or downward)

of the slab is, in the presence of water, its final state is always P_{down} for the BaO termination and P_{up} for the TiO_2 one. Thus, for BaO, a unique final state with a downward polarization is obtained, regardless of whether the initial state is P_{up} or P_{down} . This initial configuration has no influence on the values of the local polarization in the final state. That means that water is able to reverse the polarization of the whole ultrathin film, as was recently evidenced experimentally for $BiFeO_3$ [19]. More importantly, this result can be used to control the polarization. In fact, by synthesizing ultrathin films of BTO with an excess of Ba, one will obtain the BaO termination and thus in a humid environment a sample that will be polarized downward, with the converse for an excess of Ti.

Following this important result, the polarization will now be analyzed in detail.

1. BaO termination

As mentioned previously, H_2O always adsorbs dissociatively on the BaO termination and stabilizes the downward polarization regardless of the initial state. Water is thus able to switch an initial upward polarization to a downward-pointing polarization on BaO termination. However, even if the polarization is always downward with water adsorbed on the BaO termination, specific behavior can be evidenced, depending on the adsorption mode. To help the discussion, the local out-of-plane polarization of the upper cell, namely, the cell in contact with vacuum or water, for each adsorption mode reported in Figs. 2 to 6 is plotted in Fig. 10, together with the downward polarized bare BaO termination, used as a reference.

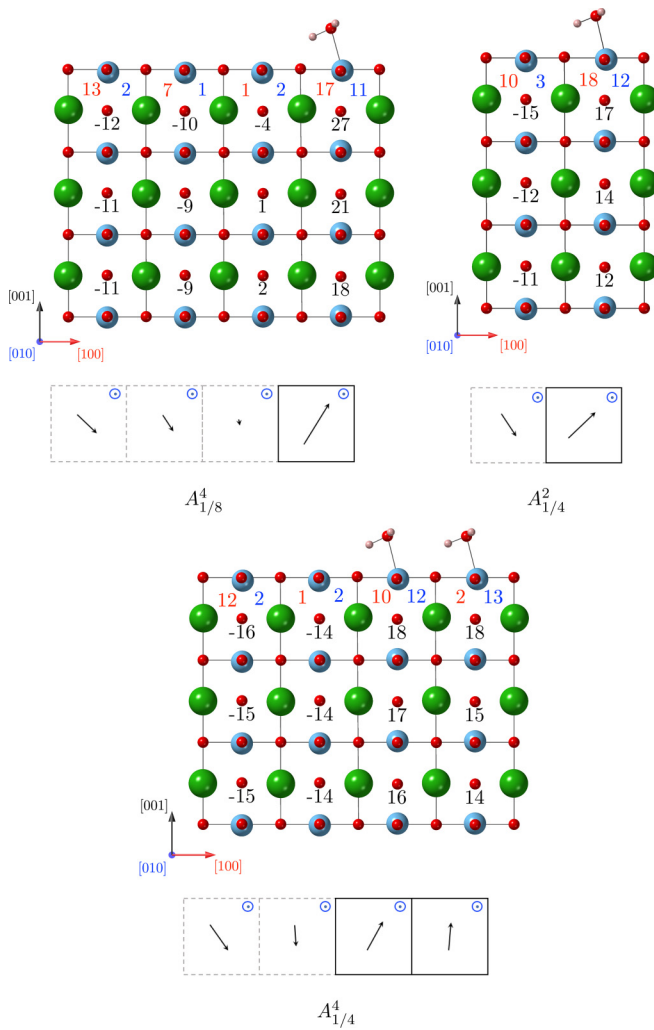


FIG. 7. Most stable structures of the TiO_2 -terminated surface with $N = 4$ and $\theta = \frac{1}{8}$ ML ($A_{1/8}^4$), with $N = 2$ and $\theta = \frac{1}{4}$ ML ($A_{1/4}^2$), and with $N = 4$ and $\theta = \frac{1}{4}$ ML ($A_{1/4}^4$). See Fig. SI7 in the Supplemental Material for the representation of the whole simulation cell.

One can first comment on the global distribution of the blue and green marks, modes 1 and 2, respectively. According to this graph, adsorption modes 1 and 2 present two distinct behaviors. Whatever the periodicity and the total number of water molecules in the simulation cell are, adsorption in mode 2 (green circles and triangles) leads to an increase of polarization in the upper cell, compared to bare BaO. On the contrary, when H_2O adsorbs in mode 1 (blue circles and triangles), the local polarization is either the same or decreased compared to BTO without H_2O . This evolution of the polarization can be directly linked to surface bondings. Indeed, for $\theta = 1/4$ ML with $N = 2$ (Fig. 3), in mode 2, the dissociated OH fragment pulls out the Ba atom by 0.26 \AA from the surface, while the surface O bound to the H fragment is pushed by 0.17 \AA in the surface. As a consequence of these surface distortions, the Ti-O bond of the upper cell is elongated. On the contrary, in mode 1 no particular distortion is observed in the first layer, and the bare BaO polarization remains. Beyond the out-of-plane polarization,

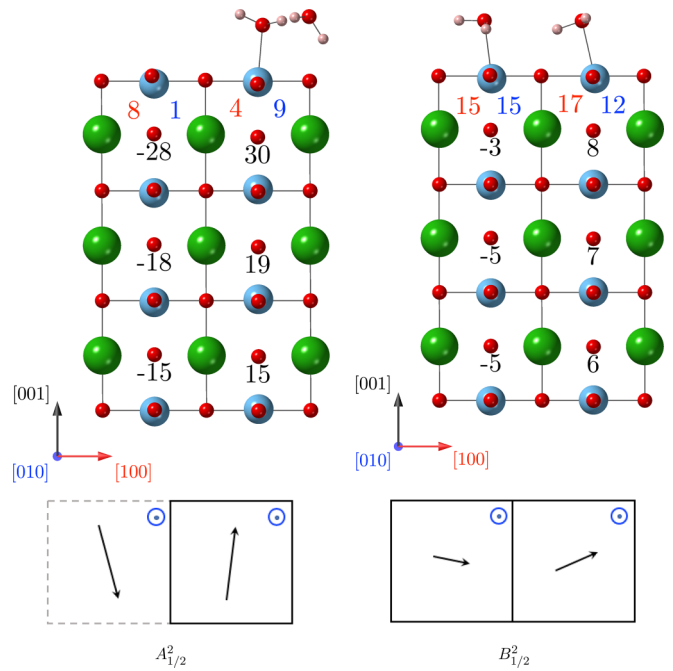


FIG. 8. Most stable structures of the TiO_2 -terminated surface with $N = 2$ and $\theta = \frac{1}{2}$ ML. See Fig. SI8 in the Supplemental Material for the representation of the whole simulation cell.

water adsorption also induces modification of the in-plane polarization. One can first comment on cases with only one water molecule per unit cell (triangles in Fig. 10). Again, modes 1 and 2 leave different imprints. Starting from an initial state without in-plane polarization, adsorption of water induces an in-plane polarization, pinned by the orientation of OH groups. When the water molecule adsorbs in the (010) plane (mode 2), an in-plane polarization arises along the [100] direction. On the contrary, for adsorption in mode 1, a small polarization appears along the [010] direction. Finally, if we compare \mathbf{P} along [100], [010], and [001] for the different periodicities reported in Figs. 2, 3, and 6, differences are observed only between the periodicities $N = 2$ and $N = 4$. Indeed, while no polarization is observed along [100] for mode 1 for the two-unit-cell periodicity (Figs. 3 and 6), a component along [100] appears for the four-unit-cell periodicity (Figs. 2 and 4), induced by the enlargement of the domain size, as already observed [33,37]. The effect is enhanced when water adsorbs in the [100] direction. Nevertheless, the in-plane polarization is still clearly pinned by the orientation of OH groups.

We can now focus on cases with two water molecules interacting, namely, circles in Fig. 10. The presence of two interacting molecules induces new behaviors. First of all, for a given coverage and mode, the presence of a second water molecule increases the out-of-plane polarization. This can be easily understood: the second molecule creates a hydrogen bond with the first one, pulling it even more out of the surface. Hence, effects described previously with one water molecule are intensified. We first consider the $A_{1/2}^2$ configuration. In this case, the first molecule adsorbs dissociatively but neither in mode 1 nor in mode 2, while the second water molecule is chemisorbed molecularly. This leads to an out-of-

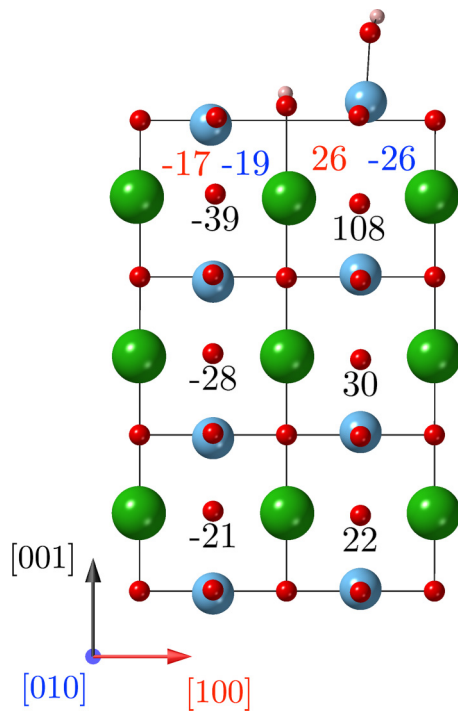


FIG. 9. Side view of the dissociative adsorption of water on the TiO_2 -terminated surface for $N = 2$ and $\theta = \frac{1}{4}$ ML. See Fig. S19 in the Supplemental Material for the representation of the whole simulation cell.

plane polarization similar to the one observed without H_2O (see Fig. 10). In addition, a small polarization appears along [010], but in the reverse direction compared to the one observed with mode 1. This modification is fully consistent with the orientation of OH groups, opposite that of mode 1.

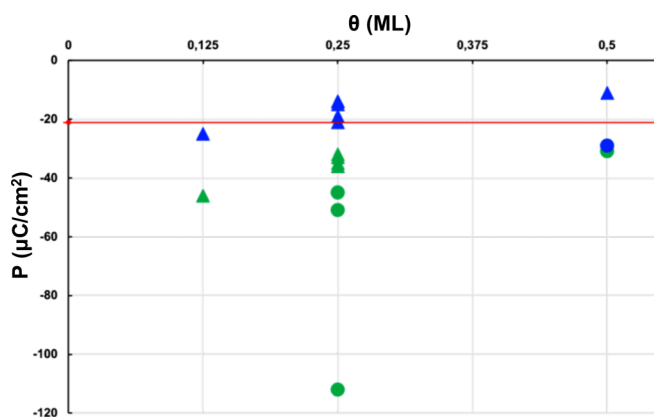


FIG. 10. Graphical representation of the local polarization (in $\mu\text{C}/\text{cm}^2$) in the upper cell (in contact with either water or vacuum) for different coverages ranging from $1/8$ to $1/2$ ML. Blue marks correspond to cases where H_2O is adsorbed in mode 1, while for green ones, water is adsorbed in mode 2. For triangles, only one water molecule is adsorbed per unit cell, while for circles two water molecules interact. Corresponding structures are reported in Figs. 2, 3, 4, 5, and 6. The red line corresponds to the reference system BaO polarized downward without H_2O .

The $B_{1/2}^2$ configuration also corresponds to one dissociated and one nondissociated water molecule. The dissociated molecule is almost along the [010] direction, as observed for mode 2. In agreement with this orientation, the polarization along [001] is increased compared to that of the bare surface. An in-plane polarization appears along the [100] direction but is a bit decreased compared to that in mode 2, while a small polarization emerges along the [010] direction. This can be explained by the orientation of the OH group. Indeed, compared to the pure mode 2, without a second molecule, OH is not perfectly aligned but slightly deviates from the [010] direction because of the hydrogen bond with the second molecule.

Finally, the last case for $\theta = 1/2$ ML ($B_{1/2}^2$) is composed of two molecules, with each one being adsorbed on a different unit cell. The neutral polarization of the whole simulation cell is almost preserved, with the dissociated molecule adsorbed on a downward polarized cell and the nondissociated physisorbed on an upward polarized cell. This repartition of adsorption configurations is consistent with polarization. Indeed, the larger dissociative adsorption leads to downward polarization. The dissociated water molecule presents a mode 1 configuration; as a consequence, a lower out-of-plane polarization is observed compared to bare BTO, and an in-plane polarization appears along the [100] direction.

2. TiO_2

As mentioned previously, we demonstrate that, on out-of-plane polarized TiO_2 -terminated BTO, the adsorption leads to upward polarization independently of the initial polarization. This polarization switching on the TiO_2 termination was suggested by low-energy electron diffraction I-V experiments in a previous study [38]. Additionally, Tian *et al.* studied the polarization switching caused by water adsorption on BiFeO_3 thin films with a FeO_2 termination [19]. They also demonstrated by means of Piezoreponse Force Microscopy (PFM) measurements that water shifted the downward polarization to an upward polarization in the whole film. Therefore, our theoretical findings demonstrating that the adsorption of water on the TiO_2 termination induces an upward polarized state in a BTO ultrathin film fully agree with previous experiments. Furthermore, in our calculations a polarization along both [100] and [010] is found in the first surface layers for all periodicities. This in-plane polarization does not exist for bare BTO, regardless of what the periodicity along [010] is, and exists only for $N = 4$ along [100], but to a lesser extent. Thus, the in-plane polarization is clearly induced by the presence of water. In addition, this is qualitatively consistent with previous results obtained by Geneste and Dkhil [20], even if a quantitative comparison is not straightforward given the differences in coverage.

Let us now focus on the out-of-plane polarization. According to Fig. 11, the presence of H_2O keeps or increases the polarization along [001]. Both the appearance of an in-plane polarization and the evolution of the out-of-plane polarization are directly related to the way the water molecule adsorbs. Indeed, the bonding between the oxygen of the water molecule and Ti pulls the Ti out of the surface up to 0.1 \AA , while the highest value observed without H_2O is 0.03 \AA for $N = 4$. As

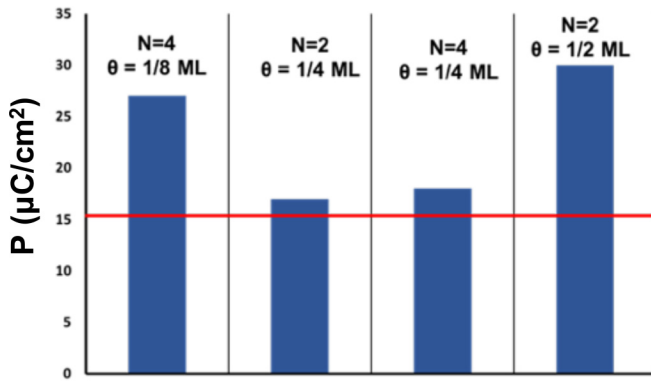


FIG. 11. Graphical representation of the local polarization (in $\mu\text{C}/\text{cm}^2$) of the upper cell for coverage of 1/8 ML with $N = 4$, for coverage of 1/4 ML with $N = 2$ and $N = 4$, and for coverage of 1/2 ML with $N = 2$ with both molecules in the same unit cell. The red line corresponds to the reference system TiO_2 polarized upward without H_2O .

a consequence the Ti-O bond of the first cell is elongated, increasing the upward polarization in this cell. In addition, the water molecule is tilted and creates a hydrogen bond with a surface oxygen. This bond sets the H_2O orientation and thus the polarization imprint.

Finally, one can comment on the dissociated case (see Fig. 9). As mentioned in the previous part, the dissociation of water induces a very large interaction between the OH fragment and the Ti atom of the first layer. As a consequence, this creates a large Ti-O bond in the first cell and thus a very important upward polarization. The out-of-plane polarization is not the only one to be affected by the water dissociation. After dissociation, both OH fragments are oriented along the [010] direction, creating a rather large polarization along [010] of $-26 \mu\text{C}/\text{cm}^2$. At the same time, the large interaction of dissociated water with the surface also induces distortions

of the first layer (see top view in Fig. 9), creating a polarization in the [100] direction, while this polarization is normally null for the bare TiO_2 -terminated BTO with $N = 2$.

IV. CONCLUSION

The adsorption of water on out-of-plane polarized BaTiO_3 ultrathin films was studied by means of DFT calculations. The influence of the surface termination, the water coverage, and the polarization direction were analyzed. We showed that water spontaneously dissociates on the BaO-terminated surface and that it stabilizes downward polarized domains regardless of the initial polarization. In addition, the out-of-plane polarization reinforces the interaction of BaO with water. Indeed, contrary to previous results on in-plane polarized BTO, only dissociative adsorption, with higher adsorption energy, was observed. On the TiO_2 , water does not dissociate spontaneously. However, both the large adsorption energy of dissociated water and the rather small barrier for dissociation tend to indicate that the dissociated case will be the most probable in real conditions. However, whatever the nature of the adsorption, the interaction of water with the TiO_2 termination always leads to domains with an upward polarization. Hence, we demonstrated that in any case the presence of water is able to induce a given polarization according to the termination of the ultrathin film. As it is known that the reactivity of a ferroelectric material is strongly linked to its polarization direction, one could imagine favoring a specific reaction by tuning the surface termination.

ACKNOWLEDGMENTS

Calculations were performed using HPC resources from DNUM CCUB (Centre de Calcul de l'Université de Bourgogne). The authors also thank ANR for financial support through project ANR-15-CE05-PHOTO-POT and project ANR-17-EURE-0002 (EIPHI Graduate School).

-
- [1] D. Tiwari and S. Dunn, *J. Mater. Sci.* **44**, 5063 (2009).
 [2] L. Li, P. A. Salvador, and G. S. Rohrer, *Nanoscale* **6**, 24 (2014).
 [3] A. Kakekhani, S. Ismail-Beigi, and E. I. Altman, *Surf. Sci.* **650**, 302 (2016).
 [4] M. A. Kahn, M. A. Nadeem, and H. Idriss, *Surf. Sci. Rep.* **71**, 1 (2016).
 [5] Y. Yun, L. Kampschulte, M. Li, D. Liao, and E. I. Altman, *J. Phys. Chem. C* **111**, 13951 (2007).
 [6] J. Garra, J. M. Vohs, and D. A. Bonnelli, *Surf. Sci.* **603**, 1106 (2009).
 [7] S. Sanna, R. Hölscher, and W. G. Schmidt, *Phys. Rev. B* **86**, 205407 (2012).
 [8] R. Hölscher, S. Sanna, and W. G. Schmidt, *Phys. Status Solidi C* **9**, 1361 (2012).
 [9] D. Li, M. H. Zhao, J. Garra, A. M. Kolpak, A. M. Rappe, D. A. Bonnelli, and J. M. Vohs, *Nat. Mater.* **7**, 473 (2008).
 [10] M. H. Zhao, D. A. Bonnelli, and J. M. Vohs, *Surf. Sci.* **602**, 2849 (2008).
 [11] M. H. Zhao, D. A. Bonnelli, and J. M. Vohs, *Surf. Sci.* **603**, 284 (2009).
 [12] K. Garrity, A. Kakekhani, A. Kolpak, and S. Ismail-Beigi, *Phys. Rev. B* **88**, 045401 (2013).
 [13] A. Kakekhani and S. Ismail-Beigi, *ACS Catal.* **5**, 4537 (2015).
 [14] R. V. Wang, D. D. Fong, F. Jiang, M. J. Highland, P. H. Fuoss, C. Thompson, A. M. Kolpak, J. A. Eastman, S. K. Streiter, A. M. Rappe, and G. B. Stephenson, *Phys. Rev. Lett.* **102**, 047601 (2009).
 [15] J. Shin, V. B. Nascimento, G. Geneste, J. Rundgren, E. W. Plummer, B. Dkhil, S. V. Kalinin, and A. P. Baddorf, *Nano Lett.* **9**, 3720 (2009).
 [16] D. Y. He, L. J. Qiao, A. A. Volinsky, Y. Bai, M. Wu, and W. Y. Chu, *Appl. Phys. Lett.* **98**, 062905 (2011).
 [17] H. Lee, T. H. Kim, J. J. Patzner, H. Lu, J. W. Lee, H. Zhou, W. Chang, M. K. Mahanthappa, E. Y. Tsymbal, A. Gruverman, and C. B. Eom, *Nano Lett.* **16**, 2400 (2016).
 [18] O. Copie, N. Chevalier, G. Le Rhun, C. L. Rountree, D. Martinotti, S. Gonzalez, C. Mathieu, O. Renault, and N. Barrett, *ACS Appl. Mater. Interfaces* **9**, 29311 (2017).

- [19] Y. Tian, L. Wei, Q. Zhang, H. Huang, Y. Zhang, H. Zhou, F. Ma, L. Gu, S. Meng, L.-Q. Chen, C.-W. Nan, and J. Zhang, *Nat. Commun.* **9**, 3809 (2018).
- [20] G. Geneste and B. Dkhil, *Phys. Rev. B* **79**, 235420 (2009).
- [21] X. Li, B. Wang, T. Y. Zhang, and Y. Su, *J. Phys. Chem. C* **118**, 15910 (2014).
- [22] X. Li, Y. Bai, B. C. Wang, and Y. J. Su, *J. Appl. Phys.* **118**, 094104 (2015).
- [23] G. Kresse and J. Furthmüller, *Phys. Rev. B* **54**, 11169 (1996).
- [24] G. Kresse and J. Furthmüller, *Comput. Mater. Sci.* **6**, 15 (1996).
- [25] S. Grimme, J. Antony, S. Ehrlich, and H. Krieg, *J. Chem. Phys.* **132**, 154104 (2010).
- [26] J. P. Perdew, K. Burke, and M. Ernzerhof, *Phys. Rev. Lett.* **77**, 3865 (1996).
- [27] P. E. Blöchl, *Phys. Rev. B* **50**, 17953 (1994).
- [28] G. Kresse and D. Joubert, *Phys. Rev. B* **59**, 1758 (1999).
- [29] J. D. Pack and H. J. Monkhorst, *Phys. Rev. B* **13**, 5188 (1976).
- [30] See Supplemental Material at <http://link.aps.org/supplemental/10.1103/PhysRevB.101.075410> for figures showing the whole simulation cell, as well as additional figures showing the explicit substrate.
- [31] H. Guo, L. Liu, Z. Chen, S. Ding, H. Lu, K. Jin, Y. Zhou, and B. Cheng, *Europhys. Lett.* **73**, 110 (2006).
- [32] S. Lee, L. Baasandorj, J. Chang, I. Hwang, J. Kim, J. Kim, K. Ko, S. Shim, M. Choi, M. You, C. Yang, J. Kim, and J. Song, *Nano Lett.* **19**, 2243 (2019).
- [33] P.-M. Deleuze, A. Mahmoud, B. Domenichini, and C. Dupont, *Phys. Chem. Chem. Phys.* **21**, 4367 (2019).
- [34] M. Sepliarsky, M. G. Stachiotti, and R. L. Migoni, *Phys. Rev. Lett.* **96**, 137603 (2006).
- [35] J. D. Baniecki, M. Ishii, K. Kurihara, K. Yamanaka, T. Yano, K. Shinozaki, T. Imada, and Y. Kobayash, *J. Appl. Phys.* **106**, 054109 (2009).
- [36] G. Henkelman, B. P. Uberuaga, and H. Jonsson, *J. Comput. Phys.* **113**, 9901 (2000).
- [37] J. Dionot, G. Geneste, C. Mathieu, and N. Barrett, *Phys. Rev. B* **90**, 014107 (2014).
- [38] J. L. Wang, F. Gaillard, A. Pancotti, B. Gautier, G. Niu, B. Vilquin, V. Pillard, G. L. Rodrigues, and N. Barrett, *J. Phys. Chem. C* **116**, 21802 (2012).